Establishing a silica gel zone in well annulus and evaluating its performance in blocking vertical water flow

Lirong Zhong *, Jonathan N. Thomle, Rob D. Mackley, Zoe G. Vincent, Frederick D. Day-Lewis

Pacific Northwest National Laboratory, 902 Battelle Blvd, Richland, WA 99354, USA

ARTICLE INFO

Keywords:
Colloidal silica suspension
Gelation after injection
Silica gel
Density sinking prevention
Well annulus
Water flow blocking

ABSTRACT

Wells are often constructed for monitoring purposes with relatively long screen lengths (e.g., >10 m). Vertical water flows can occur within the artificial or natural filter pack annulus that surround the screened interval, bypassing packer assemblies installed inside the wellbore. Attempts to isolate discrete vertical zones during groundwater sampling are unsuccessful when annular vertical flow occurs which lead to remedy decisions based on biased or incorrect interpretations. Blocking vertical annular water flow and contaminant transport will help obtain more accurate concentrations of contaminants from sampling in targeted depth intervals. The application of silica gels formed from the injected colloidal silica (CS) suspensions is a novel approach to minimize or prevent vertical movement of groundwater in the surrounding filter pack annulus. In this study, we tested the feasibility of injecting CS suspensions to target locations and developed a modified CS formulation that is injectable and prevents gravity sinking. We studied the spatial distribution and penetration of silica gel at laboratory scale in model well annulus with surrounding formations. We evaluated the performance of the silica gel in blocking vertical water flow in the annulus and in minimizing chemical transport through the gel zone. CS suspension formulations have been defined that are ready for injection, persist in target locations, and form gel within desired time frames. Injection of CS suspensions achieved uniform distribution in a well annulus filter pack, fully occupied the annulus pore space, and penetrated the formation surrounding the filter packer with a sufficient distance to create a hydraulic annular seal when the injection was applied at a sufficient rate. Silica gel that formed in the annulus blocked vertical water flow and stopped the chemical transport through the gel zone. This research reveals that using CS suspension injection and sequential gelation (CS-GEL) is a promising technology for blocking vertical water flow and chemical transport through the filter pack in targeted zones within the annulus of long-screened well systems.

1. Introduction

Many long-screened wells have been constructed for monitoring purposes, such as those at the U.S Department of Energy's Hanford Site located in southeast Washington state (Day-Lewis et al., 2023; Vermeul et al., 2011). In these long-screened wells, ambient vertical flows in the wellbore can reach liters per min, even with a minimal water head difference in the well-connected aquifer layers (Poulsen et al., 2019; Vermeul et al., 2011). Wellbore mixing due to ambient vertical flows during groundwater sampling from long-screened wells may produce biased concentration results for contaminants such as nitrate, arsenic, and uranium (Day-Lewis et al., 2023; Huang et al., 2022; Vermeul et al., 2011). Attempts to isolate the unwanted groundwater flow to the sampler using a packer system inside the wellbore are effective to some extent at reducing the biases in the sample concentrations. However, groundwater can still flow around the packer system through the filter pack materials within the well annulus, as illustrated in Fig. 1. Besides causing challenges during groundwater sampling, the ambient vertical water flow in these wells also induces vertical migrations of contaminants among plumes at different depths.

Therefore, blocking the vertical water flow in existing long-screened well annulus and isolating the groundwater flow from the target aquifer layers into the monitoring wells are needed to obtain more accurate measurements of contaminant concentrations representative of the targeted layers and to improve the extraction efficiency from target aquifer formations.

* Corresponding author.
E-mail addresses: lirong.zhong@pnnl.gov (L. Zhong), rdm@pnnl.gov (R.D. Mackley), zoe.g.vincent@pnnl.gov (Z.G. Vincent), frederick.day-lewis@pnnl.gov (F.D. Day-Lewis).

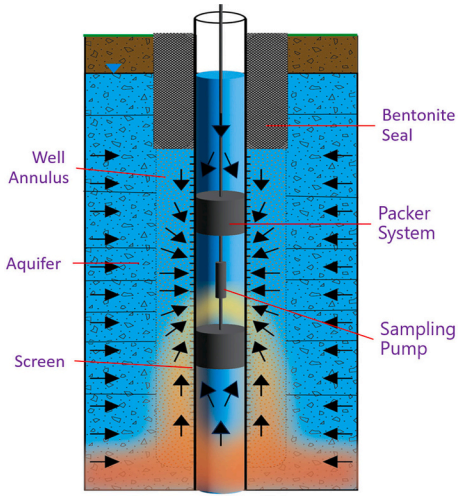

Fig. 1. Illustration of the vertical water flow around the packer system in a long-screened well annulus that causes biased groundwater sampling results. Modified from (Zhong et al., 2024).

Colloidal silica (CS) is an aqueous suspension of nano to micron-sized silica (SiO_2) particles. It has low viscosity (<10 mPa·S) even when the silica concentration reaches 30 wt%. When an electrolyte, such as sodium chloride (NaCl), is mixed with the suspension, a gelation process is initiated. In this process, the suspension has low viscosity when freshly prepared, then undergoes an increase in viscosity over time, and eventually forms a gel when the formulations of the suspensions are desirable (Katoueizadeh et al., 2020; Yang et al., 2016). The CS suspensions of fumed silica particles also exhibit shear thinning behavior in the tested shear rates ranging from 0.1 to 120 s^{-1} (Amiri et al., 2009; Chen et al., 2005; Zhong et al., 2018). The low viscosity and shear thinning properties of fresh silica suspensions promote injection of the suspensions into the subsurface. Low viscosity and small particle size in the suspension also enable increased penetration of the fluid into the injected media. After gelation, the silica gel stays at a fixed location in the subsurface to perform its desired functions such as plugging leaks and blocking flows (Ezzedine et al., 2012; Fleury et al., 2017; Hunt et al., 2013; Ngo et al., 2021; Pagano et al., 2022), grouting radioactive contaminants (Pagano et al., 2023; Truex et al., 2011), performing as a flow barrier (Durmusoglu and Corapcioglu, 2000; Kim and Corapcioglu, 2002) and enhancing hard rock formation stability in tunnel constructions(Funehag and Fransson, 2006; Funehag and Gustafson, 2008; Sögaard et al., 2018).

These suspensions are favorable candidates for this specific application of blocking the vertical water flow in well annuli given the flow and gelation characteristics of CS suspensions and their environmental benignity, such as their nontoxic nature and minimal interference to the environment. A CS suspension formulation based on a commercially available silica suspension recovered from geothermal fluids has been defined and tested for its performance in blocking vertical water flow in well annuli at the laboratory benchtop scale (Zhong et al., 2024). It has been demonstrated that this CS formulation can be successfully injected into the target zones in the well annulus, and that the formed silica gel can fully block water flow and chemical transport through the gelled zones.

In this study, we extended laboratory benchtop (centimeter) scale testing of the CS suspension reported in our earlier study (Zhong et al., 2024) to a larger intermediate (meter) scale to demonstrate that the desirable performance of a CS suspension formulation and the silica gel derived from it can be successfully upscaled. These results support field-scale implementation and performance evaluations of the CS suspension injection-and-gelation (CS-GEL) technology for blocking vertical water flow in long-screened monitoring well systems. The injection-and-gelation processes, as well as the distribution and penetration of silica gel in the well annulus, were tested. These experiments also assessed the gel's performance in blocking vertical water flow and chemical transport. Additionally, benchtop batch diffusion and rheology tests were conducted to study the characteristics of the CS suspensions and gels.

2. Materials and methods

Rheology studies, batch diffusion tests, and benchtop and intermediate scale sandbox experiments were performed in this work. The materials used and testing procedures applied are presented below.

2.1. Materials

The CS suspension, GEO-40 Sol—1030Na, was obtained from GEO40.com (Auckland, New Zealand). This CS suspension was recovered from geothermal fluids, endowing a comparatively low carbon footprint. According to the technical data provided by the vendor, this suspension contains 30.6 wt% silica particles. The measured silica particle size is 7.0–10.0 nm with an average diameter of 8.0 nm. The surface area ranged from 272 to 388 m^2/g with an average of 341 m^2/g. The pH of the suspension is 9.8.

Potassium bromide (KBr) was selected as the chemical tracer in the tests. NaCl was used as the destabilizer for the silica suspensions to initiate the gelation process. Amaranth dye was applied to color the silica suspension for the purpose of visually tracking the suspension distribution in a porous medium after injection. Xanthan gum ($C_{35}H_{49}O_{29}$ [monomer]) powder (Ingredion, Westchester, Illinois, USA), a biopolymer, was used as an additive to the CS suspensions to modify their rheological properties and to enable them to resist density sinking and persist at the target locations after injection.

Mesh 12/20 sand (#12/20 sand) was purchased (ACCUSAND®) from Covia Corp (Minnesota, USA). Mesh 16, 30, and 70 silica sands (#16, #30, #70 sands) were obtained from Lane Mountain Company (Valley, Washington, USA). Mesh 120 high purity silica sand (#120 sand) was provided by Teton Supply Co. The hydraulic conductivities, measured using constant head permeability test method, were 604.9, 513.7, 343.3, 18.3, and 6.4 m/d for the #16, #12/20, #30, #70, and #120 sands, respectively. Hanford Site simulated ground water (SGW) was prepared based on previously described method (Emerson et al., 2017), to saturate the porous media in the Phase-II sandbox tests.

2.2. Experimental setup and test procedures

2.2.1. Rheology tests

The viscosity and rheology measurements on the CS suspensions before and after NaCl and xanthan gum addition were conducted using an Anton Paar Physica MCR302 rotational rheometer (Anton Paar Inc., Ashland, Virginia, USA). A cup-and-spindle measuring system, CC27, was used for the rheology flow curves measurements with shear rates between 0.1 s^{-1} and 150 s^{-1}. A built-in temperature control chamber allowed selection of the desired experimental temperature (20 °C ± 0.1 °C).

2.2.2. NaCl release from silica gel tests

NaCl release tests were conducted in a batch system. A cylindrical-shaped silica gel formed from CS suspension containing 18 % SiO_2 and 7500 mg/L Na^+ (from NaCl) with a diameter of 2.7 cm and a length of 5.5 cm was placed into 700 mL of SGW contained in a beaker. The electrical conductivity of the water was measured over time for 9000 min (150 h) using a conductivity meter (HACH, Loveland, Colorado, USA). The water was gently mixed with a stir bar during the sampling period (Fig. S1). The NaCl concentrations in the water were determined using the electrical conductivity values based on a calibration. The rate of NaCl diffusion from the gel was then calculated using the NaCl concentration change in the water. Two batch release tests were conducted,

one with a fresh silica gel, and the other with silica gel aged for 55 days.

2.2.3. Sandbox test setup

A set of sandbox experiments were conducted as summarized in Table 1. Sand boxes were designed at varying scales, experimental complexity, and materials to evaluate CS gel performance under scenarios with varying physical and hydrologic conditions. They were designed to simulate long-screened groundwater wells surrounded by annular (e.g., filter pack sand) and aquifer materials representative of those found in the field.

Previous benchtop scale tests were conducted in which a scaled well screen was surrounded only by annular filter pack material to test the CS injection and the vertical flow blocking performance of the formed gel (Zhong et al., 2024). Following the previously described tests, the benchtop-scale sandbox tests (Phase-I) and intermediate scale sandbox tests (Phase-II) were performed in this study (Table 1) to evaluate the establishment of CS gel zones and test their performances in blocking vertical water flow. The components, dimensions, and the porous media packing patterns of the Phase-I and Phase-II sand boxes are illustrated in Fig. 2. To observe the distribution of the injected CS suspension with dye, the outside wall of the Phase-I sandbox was built with a 6″ (15.2 cm) nominal diameter transparent polyvinyl chloride (PVC) pipe (schedule 40). The Phase-II sandbox was built with a 24″ (57.0 cm) nominal diameterPVC (schedule 40) pipe. The wells for Phase-I and Phase-II were constructed using 2″ (5.08 cm) nominal diameter slotted PVC (schedule 40) screens with 0.02″ (0.05 cm) slot openings. The complete Phase-II set up is presented in Fig. S2.

2.2.4. Sandbox test procedures

Test the persistence of CS suspension in target location after injection: The sandbox from (Zhong et al., 2024) was used in this testing. Two tests were conducted to evaluate the behavior and distribution of CS following emplacement, one injecting the CS suspension alone and the other injecting the CS suspension with 2500 mg/L of xanthan gum. The injected volume was 300 mL in each test, and injection rates were 150 mL/min in both tests. The injection locations in the #12/20 sand were the same in the two tests. Amaranth dye was added to both suspensions at a concentration of 200 mg/L, thus, the injected fluid could be seen inside the sandbox. Repeat photos were taken to record the distribution and any migration of the CS within the injection zone over time following emplacement. Suspensions with and without xanthan gum addition were compared.

Test CS injection, gel distribution and penetration, water flow blocking: Phase-I and II sandbox tests were performed with procedures including the following steps.

i) Sediment Packing

The Phase-I and II sandbox tests were packed with sands to form the patterns shown in Fig. 2. A pipe with outer diameter of either 10.2 cm or 16.8 cm was placed at the desired elevation on top of the #12/20 or #16 sand over the center well pipe in Phase-I and Phase-II experiments, respectively. This pipe allowed two different sand materials to be packed within the same sandbox to form the annulus (inner packing) and the formation (outer packing). For each packing the pipe was moved upward in a stepwise fashion, while the porous media was gradually packed on both the inside and outside of the pipe to fill the sandbox.

ii) Pre-CS Injection Hydraulic Conductivity and Tracer Test

Once packed, the porous media were saturated with Hanford Site SGW (Phase-I) or tap water (Phase-II). A rubber plug was inserted into the well at the location indicated in Fig. 2. Water was injected from the port at the bottom of the sandbox at flow rates ranging from 3.0 to 200 mL/min for Phase-I, and from 0.5 to 5.0 L/min for Phase-II tests, respectively, to test the hydraulic conductivity of the sand packs. The injection pressure was recorded with the effluent port of the sandbox open to the air, allowing free water flow. In the Phase-I sandbox tests, a tracer test was also conducted by injecting 15 mL of the chemical tracer KBr at a concentration of 5000 mg/L into the annulus sediment above the rubber plug. After injecting the tracer, liquid samples were taken from the wellbore at locations above and below the plug, as shown in Fig. 2(A). Each tracer test lasted for 10 h with sampling intervals of 0.5 h, and sampling volumes of 1.5 mL. Tracer concentrations were determined using a bromine (Br) ion electrode (Accumet Materials Co LLC, New York, USA) based on a calibration between the electrode reading and the Br^- concentration.

iii) CS Suspension Injection and Gelation

For the injection of the CS suspension, the rubber plug inside the well was replaced with a unit built for injection into the annulus. The injection system was made up of a 6.35 mm diameter stainless steel tubing with a perforated section 5.7 cm long for Phase-I and 8.0 cm long for Phase-II. The perforated section was bounded within the well pipe between two rubber plugs to isolate the injection zone and force the CS suspension flow radially through the well screen into the annulus. In the Phase-I and Phase-II tests, 140 mL and 1300 mL of a CS suspension with dye were injected, respectively. The injected suspensions were allowed for overnight gelation.

iv) Post-CS Injection Hydraulic and Tracer Test

After gelation, the injection unit was replaced with the rubber plug, and a tracer test was conducted following the same procedure described above for Phase-I tests. When the CS suspension injection unit was pulled out from the well, the silica gel remaining inside the wellbore from the injection process was removed. A set of water injection tests was conducted in both Phase-I and Phase-II to determine the hydraulic conductivity of the sand pack system with silica gel by reinserting the rubber plug into the well at the location indicated in Fig. 2. Water was again injected from the port at the bottom of the sandbox at flow rates ranging from 3.0 to 200 mL/min and from 0.5 to 5.0 L/min for Phase-I and Phase-II tests, respectively. The injection pressure was recorded with the effluent port of the sandbox open to the air, allowing free water flow.

v) Excavation

Finally, water was drained from the sandbox, and the loose sand was excavated to reveal the distribution and penetration of silica gel in the sand packs. Photographs were taken and measurements on gel blocks' dimensions were carried out during the excavation.

Table 1
Summary of sandbox experiments.

Test	Test scale and Setup	Sand Pack
Gravity sinking test	Benchtop scale (Zhong et al., 2024; Fig. 2A)	#12/20 sand
Phase-I, I-Test-01	Benchtop scale (Fig. 2A)	#12/20 sand; #30 sand
Phase-I, I-Test-02	Benchtop scale (Fig. 2A)	#12/20 sand; #70 sand
Phase-I, I-Test-03	Benchtop scale (Fig. 2A)	#12/20 sand; #120 sand
Phase-II, II-Test-01	Intermediate scale (Fig. 2B)	#16 sand; #30 sand
Phase-II, II-Test-02	Intermediate scale (Fig. 2B)	#16 sand; #70 sand
Phase-II, II-Test-03	Intermediate scale (Fig. 2B)	#16 sand; #120 sand

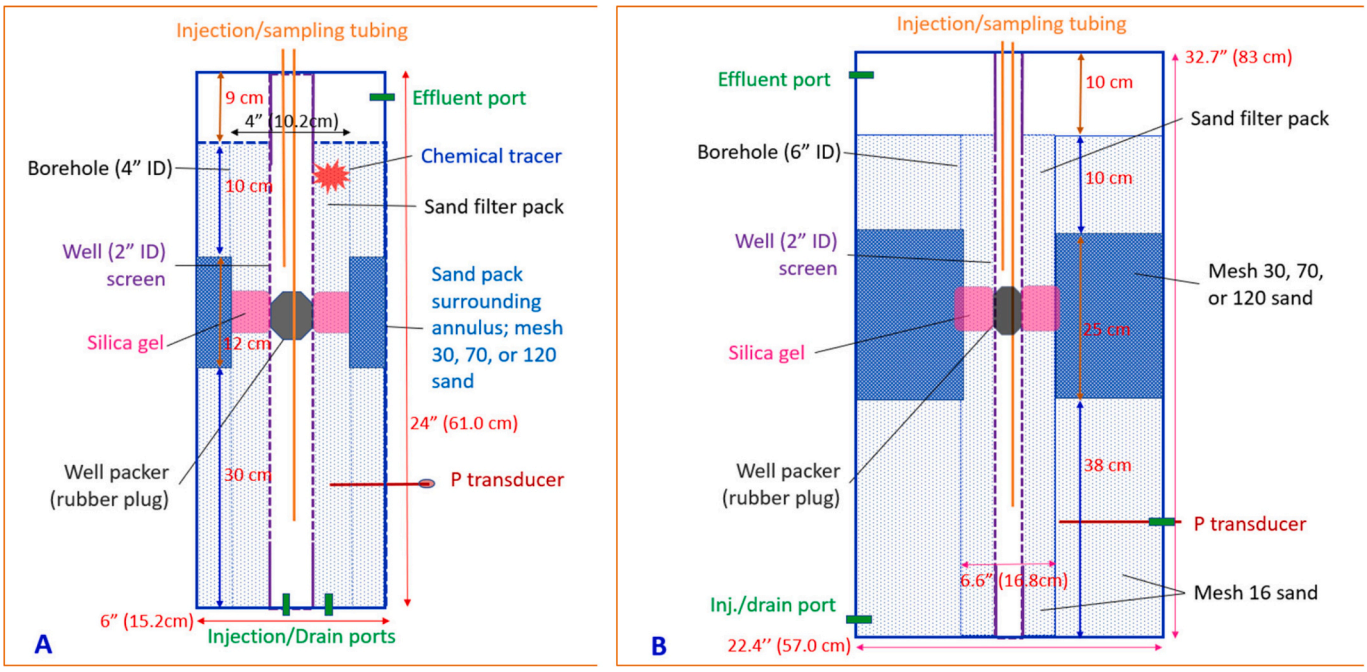

Fig. 2. Cross sections of the Phase-I (A) and II (B) sandboxes illustrating the dimensions and porous media packing patterns. Sandbox packing for both phases consisted of #16 sand packed in the well annulus and the formation material surrounding the annulus in the lower and upper portions of the sandbox (light blue filled areas). Finer-grained layers of sand (i.e., #30, #70, or #120) were placed around the annulus to represent a layer of lower-permeability formation (blue filled area). The colloidal silica (CS) suspension injection zone was located nominally in the middle of the lower-permeability sand (i.e., #30, #70, or #120) pack layer. A pressure transducer was installed below the CS suspension injection zone and an injection port was set up at the bottom of the sandbox. (For interpretation of the references to color in this figure legend, the reader is referred to the web version of this article.)

3. Results and discussion

3.1. Formulation of silica suspension to remain in the target location

The density of the CS suspension containing 18 wt% SiO_2 was 1.12 g/mL. The suspension sank quickly (in min) after being injected into the sand pack saturated with water of 1.00 g/mL density due to buoyancy-driven flow (Fig. 3[A]). In 10 min, the suspension had sunk 23 cm, a distance of more than 3 times of the injection zone height of 7.0 cm.

In order to prevent vertical water flow within the annulus of a well at a specific depth, it is critical that the injected CS suspension stays in a targeted location. Therefore, it is critical that the injected CS suspension overcomes gravity sinking. Xanthan gum, an environmentally benign water-soluble biopolymer, was added to the CS suspension at a concentration of 2500 mg/L to increase the viscosity, thus enabling the fluid to stay in the target location. The modification to the CS suspension formulation successfully prevented gravity sinking and kept the fluid at the target location, as demonstrated in Fig. 3(B). Minimal suspension sinking was observed after the formulation modification, which did not change the density of the fluid. The vast majority of the suspension stayed in the target zone 360 min after injection.

Gravitational instability of two miscible fluids in porous media will trigger convection of these fluids, normally referred to as density-driven flow (Holzbecher, 1998). Brine saturated with carbon dioxide (CO_2) was

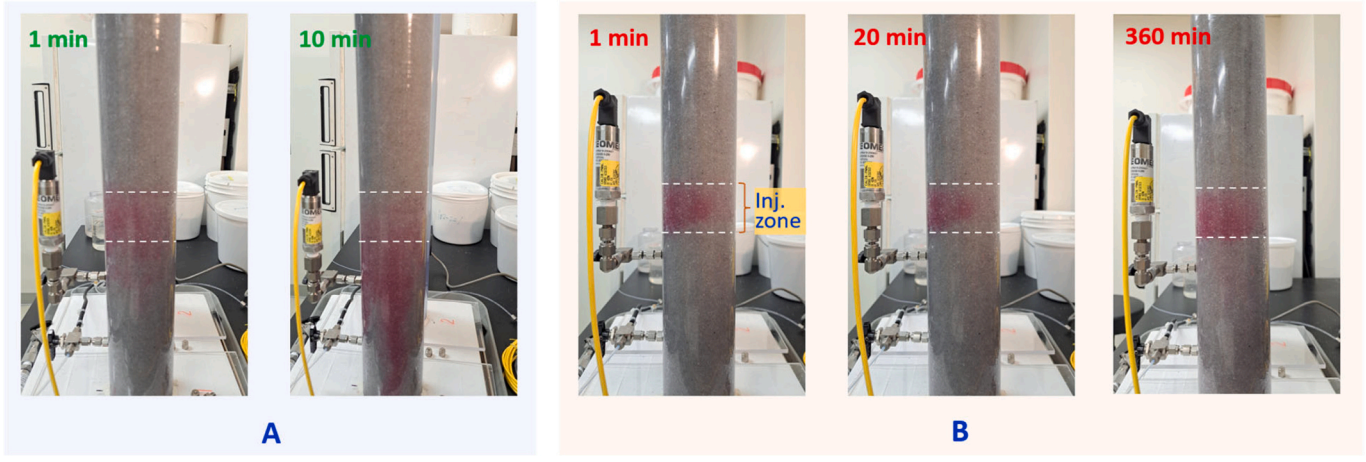

Fig. 3. Photographic comparisons showing density effects of the injected colloidal silica (CS) suspension without and with a xanthan gum additive. The dashed white lines in each photo indicate the top and bottom of the injection zones. (A) Photos were taken at 1 and 10 min after injection without the additive, revealing rapid sinkage of the suspension. (B) Photographs were taken at 1, 20, and 360 min after injection of a CS suspension with a xanthan gum additive, revealing the CS suspension stayed in the targeted location.

observed to sink into CO_2-free brine because the dissolution of CO_2 into water increased its density, which is a favorable process in geological carbon sequestration (Vermeul et al., 2011). Laboratory observation revealed that when the viscosity contrast between two miscible fluids was increased, the mobility of the fluids in the density-driven flow was reduced, retarding the convective mixing (Chen et al., 2023; Teng et al., 2020). Thus, increasing the viscosity of the CS suspension should minimize density sinking in the groundwater.

When 2500 mg/L xanthan gum was added to the CS suspension, the quasi-static viscosity of the suspension increased from 7 mPa·s to 3700 mPa·s (Fig. 4). This increase in viscosity enabled the suspension to stay in the injected location, overcoming the density sinking, as demonstrated in Fig. 3(B), since no shear was applied to the fluid when injection was stopped. In addition to increasing viscosity, the addition of xanthan gum transformed the suspension from a Newtonian fluid into a shear thinning fluid (Zhong et al., 2024) (Fig. 4). At low shear rate (e.g., 0.1 s^{-1}), the viscosity increase compared to the unmodified suspension was more than 525 times, reaching 3700 mPa·s. In the middle of the tested shear rate range (e.g., 75.0 s^{-1}), the viscosity dropped to 55 mPa·s. Finally, at the high end of the tested shear rate range (e.g., 150.0 s^{-1}), the viscosity further dropped to 40 mPa·s. At this viscosity, the fluid is ready for injection into the porous media conventionally packed in the well annulus. Besides, the shear thinning characteristic of the CS suspension would increase its injectability by improving the injection into lower-permeability zones (Truex et al., 2015; Zhong et al., 2008).

Besides demonstrating the shear thinning property of the CS suspension, the rheology measurements also revealed the gelation process induced by the addition of Na^+ to the suspension and demonstrated that the gelation process was not negatively affected by the addition of xanthan gum. When no Na^+ was added to the suspension, the fluid maintained the same viscosity over 4 h. When 7500 mg/L Na^+ was added to the suspension, the viscosity of the suspension decreased initially, which is a commonly reported phenomenon (Zhong et al., 2013). However, the viscosity increased over time. At 4 h after the Na^+ addition, the viscosity increased by more than 2 orders of magnitude at low shear rates (Fig. 4), confirming that the suspension had undergone gelation.

In summary, the addition of xanthan gum polymer to the CS suspension enables it to remain at the target location by overcoming the density effects, which is a novel approach. First, the modification increases the viscosity at a very low shear rate, i.e., when the fluid is at a quasistatic state, meaning the suspension can stay in the target location after injection. Second, at a shear rate of 75 s^{-1} and higher, which is normally reached during field injections (Skauge et al., 2018), the viscosity reduces significantly to around 42 mPa·s, enabling an effcient suspension injection. Third, the additive does not prevent the CS suspension from transforming into a gel.

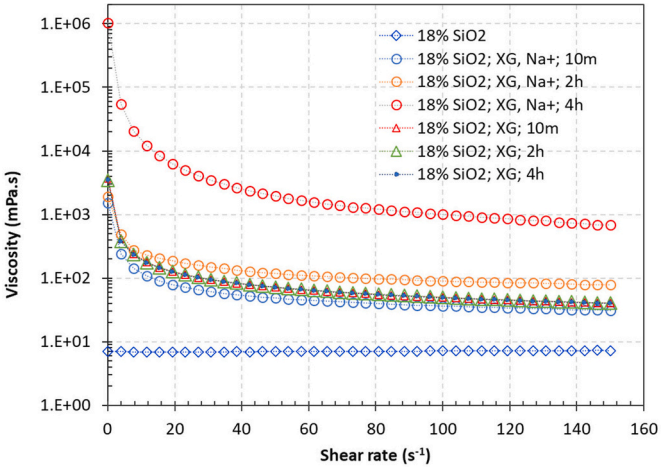

Fig. 4. Viscosity of silica suspension with and without xanthan gum (XG) and Na^+. The XG concentration was 2500 mg/L, and the Na^+ concentration was 7500 mg/L. All measurements were conducted at 20 °C with shear rate ramping from 0.1 to 150 s^{-1} completed in 30 min.

3.2. *Silica suspension injection, distribution, and penetration into surrounding sediments*

Excavation of the sandboxes at the end of the Phase-I and II tests provided an ability to directly assess the distribution of the silica gel, the shape of gel-grouted sand pack, and the penetration of the CS suspension into sand formation surrounding the annulus. Within the injection interval, the sand packed in the annular space was glued to the outside surface of the injection well of the sandbox by the silica gel (Fig. 5[A]). Removal of loose sand surrounding the gelled zone exposed the shape of the gelled sand pack (Fig. 5[A] right). The amaranth-dyed CS suspension fully occupied the pore spaces in the annular space as indicated by the red color of the annulus (Fig. 5[B]). When the gelled sand pack was detached from the well and cut in half, the cross section of the gelled sand pack showed that a layer of the sand surrounding the annular sediment was gelled together with annular sand (Fig. 5[C]), indicating the CS suspension penetrated beyond the annulus and into the surrounding formation material during injection.

When loose sand was removed from the gelled sand block, the shapes of the gelled sand blocks were revealed. In Phase-II sandbox tests, the gelled block and the well were taken from the sandbox and set on the benchtop and the dimensions of the gelled sand blocks were measured (Table 2.). In Phase-II tests, the gelled sand blocks were photographed. The dimensions were determined based on the photos (Table 2.).

All the gelled sand packs resulted in a cylindrical drum-shaped configurations (Fig. 6). A continuous layer of the surrounding #30, #70, and #120 sands for II-Test-01, II-Test-02, and II-Test-03, respectively, was gelled onto the annulus sand on the drum skin (Fig. 6, top panel of photographs). A continuous layer of #30 sand was gelled onto the drum skin in III-Test-01. About half of the drum skin area was covered by #70 sand in III-Test-02. No #120 sand was seen on the drum skin in III-Test-03 (Fig. 6, bottom panel of photographs).

The penetration distances of the gel at varying injection rates and particle size of the sand surrounding the annulus were calculated from measurements of the excavated gelled sand packs (Table 2). Penetration distances into the surrounding sand ranged from 0 to 1.37 cm. Intuitively, increased penetration distances were observed in scenarios with higher injection rates and coarser sand materials. For II-Test-02, the distance was calculated as if the gel penetrated the surrounding sand all around the annulus circumference. In II-Test-03, no penetration into the surrounding formation was observed, likely due to the insufficient flow rate.

The finer-grained sand has relatively lower permeability, explaining the lower penetration distances observed. Instead of penetrating radially into the finer-grained sand, the injected CS suspension flowed upward and downward within the annulus. Measured heights of the gelled sand packs were inversely related to the grain size of the surrounding sand pack (Table 2). Both the injection rate and the permeability contrast between the annulus sand and the surrounding sand pack play important roles in controlling the distribution and penetration of the CS suspension into the surrounding formation. Based these results, if increased penetration distances into the surrounding formations are desired to achieve more complete vertical water flow blocking, relatively higher injection rates are to be implemented in field-scale CS injections into long-screened wells (e.g., finer-grained or lower-permeability materials surround the annulus).

During the CS suspension injection, a fluid with higher viscosity displaced a fluid with lower viscosity, forming a stable displacing front (Jiao and Hötzl, 2004; Zhong et al., 2008). This stable displacing front likely explains the smooth surfaces of the gelled sand packs.

Notably, after the CS suspension was injected, the injection system

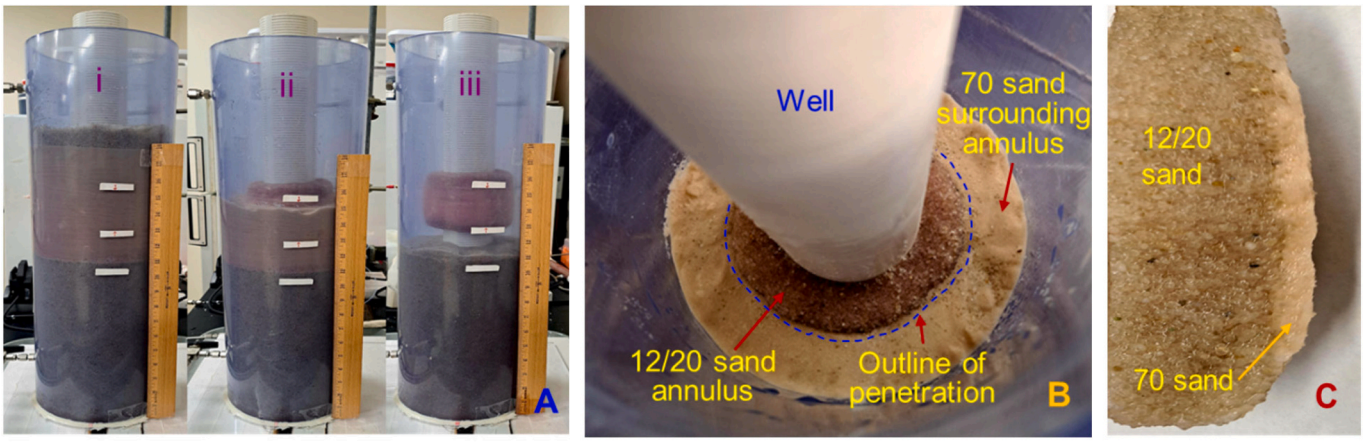

Fig. 5. Silica gel distribution and penetration. (A) Sandbox excavation. Photographs [i], [ii], and [iii] show the progression of loose sand removal from the sandbox. (B) Inside the sandbox during its excavation used in experiment Phase-I-Test-02. The injected CS suspension completely filled the pore space of the #12/20 sand in the annulus. The penetration of suspension into the #70 sand is indicated by the dashed line. (C) Cross section of the gel-grouted sand pack, indicating that the CS suspension injected through the annulus penetrated the surrounding lower-perm #70 sand pack as revealed by the grouting of #70 sand onto the annulus #12/20 sand.

Table 2
Gelled sand pack dimensions and gel penetration distance.

Test	Sand pack Annu/surrd*	Hydraulic conductivity Annu/surrd (m/d)	Injection Rate** (mL/min/cm^2)	Diameter (cm)	Height (cm)	Average Penetration Distance (cm)
I-Test-01	12–20/30	513.7/343.3	0.82	12.9	11.53	1.37
I-Test-02	12–20/70	513.7/18.3	0.82	11.05	11.84	0.43
I-Test-03	12–20/120	513.7/6.4	0.82	10.58	12.47	0.19
II-Test-01	16/30	604.9.7/343.3	0.71	17.74	16.13	0.47
II-Test-02	16/70	604.9/18.3	0.71	17.08	17.60	0.14
II-Test-03	16/120	604.9/6.4	0.71	16.19	17.93	NA

* Annu/surrd.: annulus space/surrounding formation.
** Injection rate is expressed as the flow rate of the injected CS suspension at the annulus-surrounding sand interface.

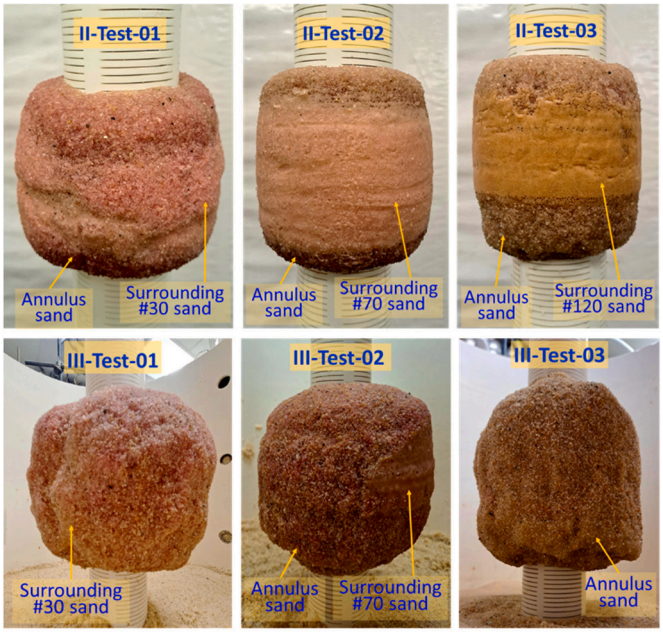

Fig. 6. Gelled sand packs that formed in the well annulus were glued on the well's outside wall by silica gel. A complete circle of sand surrounding the well annulus was gelled onto the annulus sand pack in experiments I-Test-01, 02, 03, and II-Test-01. About a half circle of the surrounding sand was gelled onto the annulus sand pack in II-Test-02. No surrounding sand was grouted on the annulus sand pack in II-Test-03.

was kept inside the well and no water flushing was applied to replace the suspension contained in the system. When the injection system was pulled out from the well, the gel formed in the well was removed together with the injection system (Fig. S3). The CS suspension fully filled the space between the two rubber plugs of the injection unit. Some suspension flowed through the annular sand pack onto the wellbore on top of the upper rubber plug and formed gel there. The silica gel was detached from the inside wall of the well and removed as a whole piece. It is expected that the gel formed in the injection well can also be removed from the well during field application when a similar procedure is applied.

3.3. Reduced annular flow with CS gel treatment

Flow testing was performed before and after CS injections to evaluate the reduction in annular vertical flow across the treated zone. The observed increase in differential pressure with increasing flow rates are shown in Fig. 7 for selected Phase-I and Phase-II test scenarios. Higher pressure buildup for a given flow rate is observed for each of the six treated test cases vs. the untreated case. Higher pressures are also associated for the test cases with finer-grained surrounding sand materials, as might be expected.

The calculated regression-line slopes from the Phase-I tests were 0.23, 0.40, and 0.87 [psi/(ml/min/cm^2)] for I-Test-01 (#30 sand), I-Test-02 (#70 sand), and I-Test-03 (#120 sand), respectively. In comparison, the slopes in Phase-II tests were 0.06, 0.40, and 0.59 psi/(ml/min/cm^2)] for II-Test-01 (#30 sand), II-Test-02 (#70 sand), and II-Test-03 (#120 sand), respectively.

Flow testing results suggest the effective hydraulic conductivity of the combined annulus and surrounding formations was decreased by the

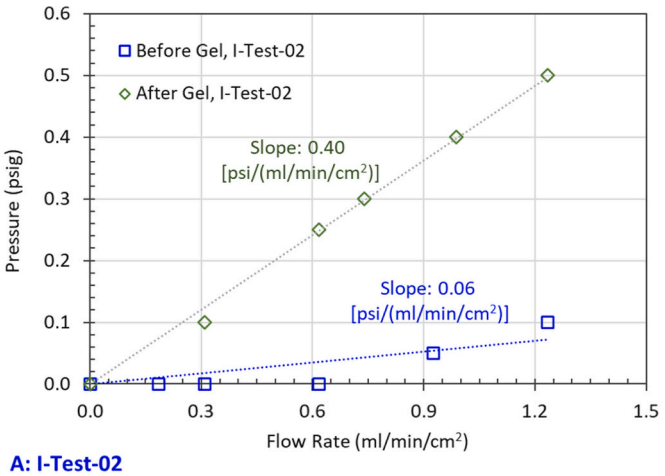

A: I-Test-02

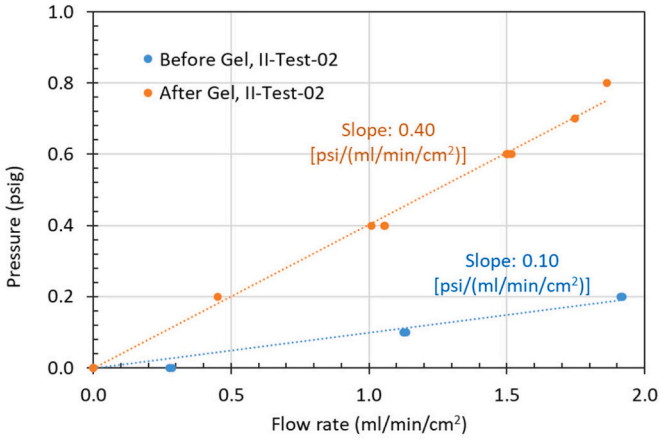

B: II-Test-02

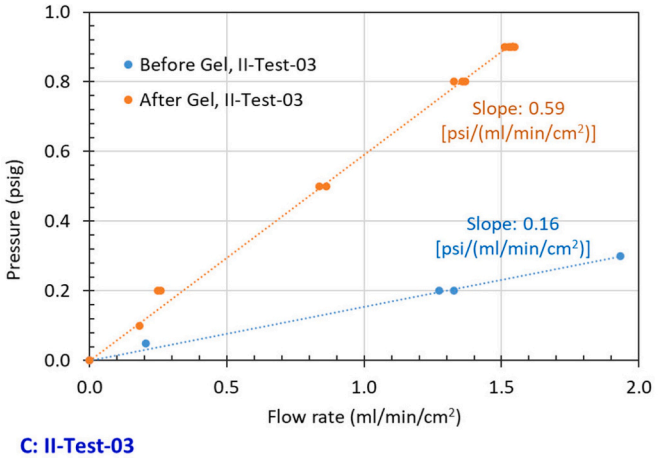

C: II-Test-03

Fig. 7. Water flow rate vs. pressure drop before and after gel is formed in the well annulus for selected tests. Flow rate is the flow on a unit cross section area of the flow pass. (A) Phase-I-Test-02. (B) Phase-II-Test-02. (C) Phase-II-Test-03.

CS treatment, even in cases where the annulus wasn't fully treated or penetration into the surrounding sand didn't occur. Pressure increases by about an order of magnitude for CS treated test cases (Fig. 7). For test cases where CS fully penetrated the surrounding sand, the injected water would likely be forced to flow laterally around the annulus and vertically through the surrounding sand causing higher differential pressures compared to the no-treatment cases. Annular bypass of flow was minimized or entirely prevented. Even in instances where the injected CS did not treat the annulus fully and/or penetrate into the surrounding sand (e.g., II-Test-02 and II-Test-03), pressures were higher in the treated cases, albeit they offer less hydraulic resistance compared to the fully-treated cases.

A noted limitation of this test setup is that flow and pressure values reflect the combined annulus-surrounding sand flow system and do not isolate flow solely within the annular treatment zone. Despite this limitation, these results provide a qualitative indication that CS treatment increases hydraulic resistance to flow by about an order of magnitude (7 ×) even under relatively high hydraulic gradient conditions (0.1 to 0.9 cm/cm).

3.4. *Tracer transport through gel zone*

A series of chemical tracer tests were performed, using a non-reactive Br^- solution, to further evaluate the performance of CS treatment for minimizing or reducing the exchange of groundwater through the annulus. The tracer was quickly released into the annulus within the upper portion of the sandbox. A rubber plug, installed inside the wellbore, prevented injection and advective transport of the tracer inside the wellbore (as shown in Fig. 2). Once released, the tracer was allowed to migrate within the annulus and surrounding sand via dispersive transport processes (e.g., density and concentration gradient). Unlike the flow testing discussed above, tracer transport involved no advective flow. Water samples were taken from above and below the zone in the wellbore after tracer injection to monitor the tracer elution and breakthrough, respectively.

Fig. 8 shows the tracer elution and arrival curves for the upper and lower monitoring locations, respectively for a representative test case (Phase-I-Test-02). In the baseline untreated test case (Fig. 8[a]), the tracer concentration decreased in the upper zone rapidly within 300 min, and then continued to decrease in concentration more slowly for the remaining monitoring period. The tracer arrival and breakthrough to the lower portion of the annulus located below the targeted treatment zone and wellbore plug occurs after 100 min. It continued to slowly increase until the test time of 500 min and appeared to be slowly decrease during the remaining monitoring period. The tracer elution and breakthrough curves likely indicate faster initial tracer transport within the coarser-grained annulus (#16 sand), possibly followed by tracer additional transport within the finer-grained sand (#70 sand) surrounding the annulus.

Tracer testing in the CS treated case (Fig. 8[b]) indicate much different tracer transport behavior compared to the untreated base case (Fig. 8[a]). The tracer eludes quickly from the upper annulus portion of the sandbox, like the untreated case but less rapidly and concentrations remain about 4× higher. The tracer does not breakthrough rapidly to the lower annulus sampling location via annular flow. In fact, there is no arrival of the tracer after 10 h. Presumably, the tracer has dispersed broadly within the sand surrounding the annulus to some unknown depth in the sandbox. The tracer dispersion testing results were consistent with the advective flow testing and indicate the injected CS treatment forms an effective hydraulic annular seal.

3.5. *Leaching of NaCl from CS gel*

Tests were performed to assess the leachability of the CS suspension and subsequent silica gel. Leaching of NaCl from the CS gel may have undesirable effects on water quality and sampling interference in field applications. The silicon dioxide (SiO_2) particles are engaged in the 3-D network of the gel (Iler, 1979; Vinogradova et al., 2006), and therefore remain in the system after gelation and not a concern. However, the NaCl added to the CS suspension to initiate the gelation is likely to be fully released from the gel and leaching rate needs to be evaluated prior to possible field implementation. Test results indicate that the rate of the NaCl release exponentially decreased over time. In 150 h, the NaCl release rate approached near zero (Fig. 9). Aging of the silica gel up to

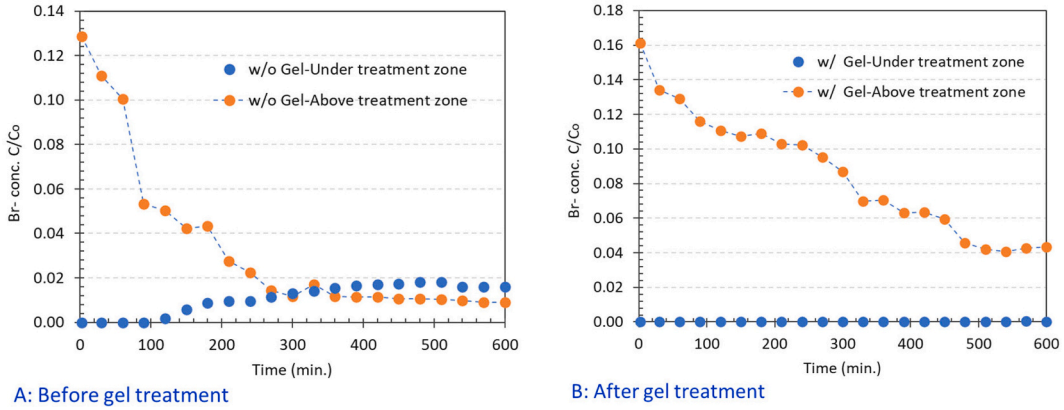

Fig. 8. Chemical transport blocked. Plots are from I-Test-02. C = observed concentration; C_o = concentration of the injected tracer solution. (A) No silica gel was formed in the sandbox system, and the tracer was transported from above the "gel zone" through to the section below. (B) Silica gel was formed in the sandbox system, and tracer injected above the gel zone was not detected in the wellbore below the gel-treated zone.

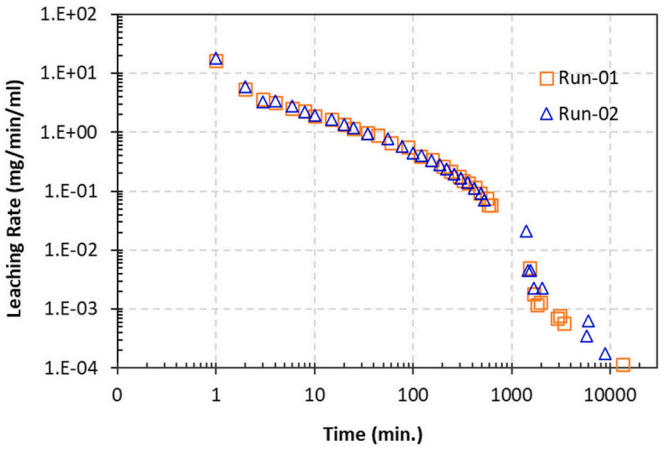

Fig. 9. Leaching rate of sodium chloride from the silica gel into simulated ground water. Run-01 used a freshly prepared silica gel; Run-02 used a gel aged for 55 days.

55 days did not affect the NaCl release rate.

Silica gel has been studied as a slow-release source for remedial amendment. The rate of release for permanganate MnO_4^- into batch water from silica gel formed from colloidal silica particle suspensions has been reported (Ogundare, 2021; Yang et al., 2016; Lee and Gupta, 2014). Comparable to the NaCl releases described above, those studies showed relatively quick MnO^{4-} release at the beginning of gelation followed by an exponential decay in the release rate over time..

Chromium (Cr^{6+}) diffusion through silica gel was studied by Tantemsapya and Meegoda (2004) to evaluate the effectiveness of using this gel as a barrier to contain subsurface contamination (Tantemsapya and Meegoda, 2004). They reported that the downstream concentration of Cr^{6+} diffused through a 5 cm thick gel was 0.091 % of the upstream concentration after 400 h. When the diffusion time was less than 200 h, contaminant concentration after being diffused through the gel zone was not detectable. The diffusion coefficient was reduced when the SiO_2 concentration in the silica gel was increased. They also found that when the gelation time was over 3 h, the Cr^{6+} diffusion coefficient did not change over time, which agrees with the finding of this study related to the diffusion of NaCl from silica gel.

Although the contaminant diffusion rate through the silica gel described in Tantemsapya and Meegoda (2004) indicated that the silica gel was ineffective in containing contamination, diffusion through the gel should not affect the performance of the gel acting as a water flow blocker in a well annulus (Tantemsapya and Meegoda, 2004). Thus, diffusion of contaminants through the gel zone, typically thicker than 5 cm, should be negligible over the selected sampling durations.

It should be pointed out that after the silica gel is formed in place to block vertical water flow, the long-term cross-connection through the sand pack and surrounding formations may cause persistent influence on the monitoring zone due to diffusion (Sterling et al., 2005; Chapman et al., 2012).

4. Conclusion

The results from benchtop and intermediate scale experiments provided in this evaluation indicate CS gel can be a viable post-construction solution for addressing the unwanted vertical groundwater flow and contaminant transport into certain segments that often occurs within the filter pack or annulus of a long-screened well. In long-screened groundwater wells, vertical water flows occur within the well annulus and can bypass around wellbore packer assemblies designed to isolate a distinct target depth interval, e.g., (Ftak and Teutsch, 1990). During groundwater sampling, the water flows into the sampling zone from above and below the target sample interval and prevents a representative sample from being obtained. Minimizing or preventing flow within the annulus is essential to obtain more accurate and meaningful information on the vertical distribution of groundwater composition and contaminant concentrations within an aquifer.

The benchtop and intermediate-scale experiments provided further development and evaluation of the approach first presented in (Zhong et al., 2024) using CS suspension injections and sequential gelation (the CS-GEL technology) to block vertical water in the well annulus. A new CS formulation containing biopolymer xanthan gum has been developed, which overcomes density sinking, remains in the target location within porous media, retains good injectability, and preserves its gelation characteristics. Injection of the CS suspension achieved uniform distribution in the well annulus. When the injection rate was sufficient, the suspension completely occupied the annulus pore space and penetrated the formation surrounding the filter pack with a sufficient distance to create a hydraulic annular seal. The gel penetration depth into the surrounding formation is a function of the permeability contrast between the annulus filter pack and the surrounding formation. The silica gel that formed in the annulus stopped vertical water flow and blocked chemical transport through the gelled zone during the duration of a groundwater sampling event. The results of this research reveal that the CS-GEL technology is a promising means for blocking vertical water flow and chemical transport through the filter pack in targeted zones within the annulus of long-screened well systems.

The gel penetration into surrounding formation can play a significant role in blocking water flow from a formation into a long-screen well

system. Water flows into and mixes in the wellbore of long-screened wells, causing vertical redistribution of contaminant mass among the formation layers within aquifers. This mixing adversely affects the pump-and-treat operations efficiency, such as those being carried out at the Hanford Site. The application of the CS-GEL technology is expected to have improved efficacy in blocking water flow.

The laboratory development of the CS-GEL technology is close to complete. Modeling on the performance and preparation for field demonstration of this technology is in progress. Long-screened wells at the U.S Department of Energy's Hanford Site will be selected for the field demo.

Funding sources

This work was funded by the Deep Vadose Zone – Applied Field Research Initiative at PNNL.

CRediT authorship contribution statement

Lirong Zhong: Writing – original draft, Visualization, Methodology, Investigation, Conceptualization. **Jonathan N. Thomle:** Writing – review & editing, Methodology. **Rob D. Mackley:** Writing – review & editing, Methodology, Funding acquisition, Conceptualization. **Zoe G. Vincent:** Writing – review & editing, Methodology. **Frederick D. Day-Lewis:** Writing – review & editing, Methodology.

Declaration of competing interest

We, the authors, declare that we have no competing financial interests or personal relationships that could have appeared to influence the research work reported in this paper.

Acknowledgments

This work was funded by the Deep Vadose Zone – Applied Field Research Initiative at Pacific Northwest National Laboratory (PNNL) project. PNNL is operated by Battelle for the U.S. Department of Energy under contract DE-AC06-76RLO 1830.

The work described was performed in accordance with the PNNL Nuclear Quality Assurance Program (NQAP). The NQAP complies with U.S. Department of Energy Order 414.1D, Quality Assurance. The NQAP uses NQA 1 2012, Quality Assurance Requirements for Nuclear Facility Applications as its consensus standard and NQA 1 2012 Subpart 4.2.1 as the basis for its graded approach to quality.

Appendix A. Supplementary data

Data availability

Data will be made available on request.

References

Amiri, A., Øye, G., Sjöblom, J., 2009. Influence of pH, high salinity and particle concentration on stability and rheological properties of aqueous suspensions of fumed silica. Colloids Surf. A Physicochem. Eng. Asp. 349 (1–3), 43–54.

Chapman, S.W., Parker, B.L., Sale, T.C., Doner, L.A., 2012. Testing high resolution numerical models for analysis of contaminant storage and release from low permeability zones. J. Contam. Hydrol. 136-137, 106–116. https://doi.org/10.1016/j.jconhyd.2012.04.006.

Chen, S., Øye, G., Sjöblom, J., 2005. Rheological properties of aqueous silica particle suspensions. J. Dispers. Sci. Technol. 26 (4), 495–501.

Chen, J., Wang, G., Yang, J., Lei, T., Luo, K.H., 2023. Pore-scale study of miscible density instability with viscosity contrast in porous media. Phys. Fluids 35 (9).

Day-Lewis, F.D., Mackley, R.D., Thompson, J., 2023. Interpreting concentrations sampled in long-screened wells with borehole flow: an inverse modeling approach. Groundwater 61 (6), 834–845.

Durmusoglu, E., Corapcioglu, M.Y., 2000. Experimental study of horizontal barrier formation by colloidal silica. J. Environ. Eng. 126 (9), 833–841.

Emerson, H.P., Di Pietro, S., Katsenovich, Y., Szecsody, J., 2017. Effects of ammonium on uranium partitioning and kaolinite mineral dissolution. J. Environ. Radioact. 167, 150–159.

Ezzedine, S., Hunt, J., Bourcier, W., Robert, S., Roberts, J., 2012. Impact of silica gel development on subsurface flow and heat extraction from enhanced geothermal systems. In: Proceedings of the Thirty-Seventh Workshop on Geothermal Reservoir Engineering. Stanford University, Stanford, California.

Fleury, M., Sissmann, O., Brosse, E., Chardin, M., 2017. A silicate based process for plugging the near well bore formation. Energy Procedia 114, 4172–4187.

Ftak, T., Teutsch, G., 1990. Some new hydraulic and tracer measurement techniques for heterogeneous aquifer formations. In: Proc. Int. Conf. and Workshop on Transport and Mass Exchange Processes in Sand and Gravel Aquifers: Field and Modelling Studies. Atomic Energy of Canada Ltd., Ontario, pp. 190–197.

Funehag, J., Fransson, Å., 2006. Sealing narrow fractures with a Newtonian fluid: model prediction for grouting verified by field study. Tunn. Undergr. Space Technol. 21 (5), 492–498.

Funehag, J., Gustafson, G., 2008. Design of grouting with silica sol in hard rock – new design criteria tested in the field, part II. Tunn. Undergr. Space Technol. 23 (1), 9–17.

Holzbecher, E.O., 1998. Modeling Density-Driven Flow in Porous Media.

Huang, Y., et al., 2022. Water quality assessment bias associated with long-screened wells screened across aquifers with high nitrate and arsenic concentrations. Int. J. Environ. Res. Public Health 19 (16).

Hunt, J., Ezzedine, S., Bourcier, W., Roberts, S., 2013. Applications of Geothermally-Produced Colloidal Silica in Reservoir Management - Smart Gels. Lawrence Livermore National Lab. (LLNL). LLNL-TR-639692.

Iler, R.K., 1979. The Chemistry of Silica: Solubility, Polymerization, Colloid and Surface Properties and Biochemistry of Silica. Wiley.

Jiao, C.-Y., Hötzl, H., 2004. An experimental study of miscible displacements in porous media with variation of fluid density and viscosity. Transp. Porous Media 54 (2), 125–144.

Katoueizadeh, E., Rasouli, M., Zebarjad, S.M., 2020. A comprehensive study on the gelation process of silica gels from sodium silicate. J. Mater. Res. Technol. 9 (5), 10157–10165.

Kim, M., Corapcioglu, M.Y., 2002. Gel barrier formation in unsaturated porous media. J. Contam. Hydrol. 56 (1–2), 75–98.

Lee, E.S., Gupta, N., 2014. Development and characterization of colloidal silica-based slow-release permanganate gel (SRP-G): laboratory investigations. Chemosphere 109, 195e201.

Ngo, I., Ma, L.Q., Zhai, J.T., Wang, Y.Y., 2021. Feasibility of CO_2 as a curing agent for silicate-based grouting gel in fractures after coal mining. In: 2nd Geoscience & Engineering in Energy Transition Conference, pp. 1–5.

Ogundare, O., 2021. Optimization and Analysis of a Slow-Release Permanganate Gel for TCE Plume Treatment in Groundwater. 2021. Ohio University. Master's thesis. OhioLINK Electronic Theses and Dissertations Center. http://rave.ohiolink.edu/etdc/view?acc_num=ohiou161797021188483.

Pagano, A.G., Mountassir, G.E., Lunn, R.J., 2022. Performance of colloidal silica grout at elevated temperatures and pressures for cement fracture sealing at depth. J. Pet. Sci. Eng. 208.

Pagano, A.G., El Mountassir, G., Lunn, R.J., 2023. Colloidal silica as a grouting material for the temporary encapsulation of heat-generating radioactive waste during removal and transport operations: a proof of concept. Front. Energy Res. 11.

Poulsen, D.L., Cook, P.G., Simmons, C.T., Solomon, D.K., Dogramaci, S., 2019. Depth-resolved groundwater chemistry by longitudinal sampling of ambient and pumped flows within long-screened and open borehole wells. Water Resour. Res. 55 (11), 9417–9435.

Skauge, A., et al., 2018. Polymer flow in porous media: relevance to enhanced oil recovery. Colloids and Interfaces 2 (3).

Sögaard, C., Funehag, J., Abbas, Z., 2018. Silica sol as grouting material: a physio-chemical analysis. Nano Convergence 5 (1).

Sterling, S.N., Parker, B.L., Cherry, J.A., Williams, J.H., Lane, J.W., Haeni, F.P., 2005. Vertical cross contamination of trichloroethylene in a borehole in fractured sandstone. Ground Water 43, 557–573. https://doi.org/10.1111/j.1745-6584.2005.0087.x.

Tantemsapya, N., Meegoda, J.N., 2004. Estimation of diffusion coefficient of chromium in colloidal silica using digital photography. Environ. Sci. Technol. 38 (14), 3950–3957.

Teng, Y., et al., 2020. An experimental study of density-driven convection of fluid pairs with viscosity contrast in porous media. Int. J. Heat Mass Transf. 152.

Truex, M.J., Pierce, E.M., Nimmons, M.J., Mattigod, S.V., 2011. Evaluation of in Situ Grouting as a Potential Remediation Method for the Hanford Central Plateau Deep Vadose Zone. Pacific Northwest National Lab. (PNNL). PNNL-20051.

Truex, M.J., et al., 2015. Field test of enhanced remedial amendment delivery using a shear-thinning fluid. Groundwater Monitor. Remediat. 35 (3), 34–45.

Vermeul, V.R., McKinley, J.P., Newcomer, D.R., Mackley, R.D., Zachara, J.M., 2011. River-induced flow dynamics in long-screen wells and impact on aqueous samples. Ground Water 49 (4), 515–524.

Vinogradova, E., Estrada, M., Moreno, A., 2006. Colloidal aggregation phenomena: spatial structuring of TEOS-derived silica aerogels. J. Colloid Interface Sci. 298 (1), 209–212.

Yang, S., Oostrom, M., Truex, M.J., Li, G., Zhong, L., 2016. Injectable silica–permanganate gel as a slow-release MnO_4^- source for groundwater remediation: rheological properties and release dynamics. Environ Sci Process Impacts 18 (2), 256–264.
Zhong, L., Oostrom, M., Wietsma, T.W., Covert, M.A., 2008. Enhanced remedial amendment delivery through fluid viscosity modifications: experiments and numerical simulations. J. Contam. Hydrol. 101 (1), 29–41.
Zhong, L., Oostrom, M., Truex, M.J., Vermeul, V.R., Szecsody, J.E., 2013. Rheological behavior of xanthan gum solution related to shear thinning fluid delivery for subsurface remediation. J. Hazard. Mater. 244-245, 160–170.
Zhong, L., Lee, B., Yang, S., 2018. Establishing vadose zone slow-release carbon sources for enhanced bioremediation using silica suspension. Vadose Zone J. 17 (1), 1–10.
Zhong, L., Mackley, R., Li, L., Thomle, J., Day-Lewis, F., 2024. Applying colloidal silica suspensions injection and sequential gelation to block vertical water flow in well annulus: laboratory testing on rheology, gelation, and injection. Front. Environ. Sci. 12.